ELSEVIER

Thermochimica Acta 398 (2003) 167–174

thermochimica acta

www.elsevier.com/locate/tca

Thermal activation of copper oxide based upon the copper hydrotalcite $Cu_xZn_{6-x}Al_2(OH)_{16}(CO_3)\cdot 4H_2O$

R.L. Frost*, Z. Ding, W.N. Martens, T.E. Johnson

Centre for Instrumental and Developmental Chemistry, Queensland University of Technology, 2 George Street, G.P.O. Box 2434, Brisbane, Qld. 4001, Australia

Received 13 February 2002; received in revised form 5 June 2002; accepted 7 June 2002

Abstract

A combination of differential scanning calorimetry (DSC) and high resolution DTG coupled to a gas evolution mass spectrometer has been used to study the thermal properties of a series of Cu/Zn hydrotalcites of formulae $Cu_xZn_{6-x}Al_2(OH)_{16}(CO_3)\cdot 4H_2O$ where x varied from 6 to 0. The effect of increased Zn composition results in the increase of the endotherms and weight loss steps to higher temperatures. Evolved gas mass spectrometry shows that water is lost in a number of steps. The interlayer carbonate anion is lost simultaneously with hydroxyl units. The endotherms and differential weight loss steps were both cation and mole ratio dependent.

Keywords: Dehydration; Dehydroxylation; Hydrotalcite; Differential scanning calorimetry; High-resolution thermogravimetric analysis

1. Introduction

Much interest focuses on the use of nano-scale copper oxide for catalyst use [1–4]. The copper oxide may be used as a solid solution or as a mixture of mixed oxides. The application of these mixed oxides is in environmental applications, such as the catalytic oxidation of carbon monoxide and the wet oxidation of organics in aqueous systems. It is apparent that such metal oxide mixtures may be obtained through the formation of hydrotalcites or double layered hydroxides. These nano-scale chemicals are produced through the thermal activation of copper salts, such as copper carbonate, copper hydroxy-carbonate either synthetic or natural (malachite) and other copper salts for example copper nitrate [5–8]. Equally well, the thermally activated copper oxide materials may be obtained from the thermal activation of copper based hydrotalcites.

Hydrotalcites, or layered double hydroxides (LDH) are fundamentally anionic clays, and are less well-known and more diffuse in nature than cationic clays like smectites. The structure of hydrotalcite can be derived from a brucite structure ($Mg(OH)_2$) in which, e.g. Al^{3+} or Fe^{3+} (pyroaurite-sjögrenite) substitutes a part of the Mg^{2+} [9–11]. This substitution creates a positive layer charge on the hydroxide layers, which is compensated by interlayer anions or anionic complexes [10,11]. In hydrotalcites a broad range of compositions are possible of the type $[M_{1-x}{}^{2+}M_x{}^{3+}(OH)_2][A^{n-}]_{x/n}\cdot yH_2O$, where M^{2+} and M^{3+} are the di- and trivalent cations in the octahedral positions within the hydroxide layers with x normally between 0.17 and 0.33. A^{n-} is an exchangeable interlayer anion. In this research, we

* Corresponding author. Tel.: +61-7-3864-2407; fax: 61-7-3864-1804.
E-mail address: r.frost@qut.edu.au (R.L. Frost).

0040-6031/03/$ – see front matter © 2002 Elsevier Science B.V. All rights reserved.
PII: S0040-6031(02)00359-3

are synthesising copper based hydrotalcites of the general formulae $Cu_xZn_{6-x}Al_2(OH)_{16}(CO_3)\cdot 4H_2O$ where x varies from 6 to 0 [12]. Whilst hydrotalcites based upon $Cu_xMg_{6-x}Al_2(OH)_{16}(CO_3)\cdot 4H_2O$ have been studied, it is apparent that the Cu/Zn based hydrotalcites have not [13]. Importantly, the use of hydrotalcites in the synthesis of nanocomposites has enabled high temperature phase composite materials to be manufactured. Important to this work is the knowledge of when the hydrotalcite decomposes and the mechanisms for this decomposition. This decomposition temperature influences the temperature of the formation of this nanocomposite such that might be used for the photo-oxidation of organics in aqueous systems [14,15]. This research compliments our studies in the synthesis and characterisation of hydrotalcites [9]. In this work, we report the high-resolution thermogravimetric analysis of a series of hydrotalcites with different Cu and Zn ratios.

2. Experimental

2.1. Synthesis of hydrotalcite samples

Hydrotalcites with a composition of $Cu_xZn_{6-x}Al_2(OH)_{16}(CO_3)\cdot 4H_2O$ where x varied from 6 to 0, were synthesised by the coprecipitation method. Two solutions were prepared, solution 1 contained 2 M NaOH and 0.125 M Na_2CO_3, solution 2 contained 0.75 M Cu^{2+} ($Cu(NO_3)_2\cdot 6H_2O$) and 0.75 M Zn^{2+} ($Zn(NO_3)_2\cdot 6H_2O$) together with 0.25 M Al^{3+} ($Al(NO_3)_3\cdot 9H_2O$). Five hydrotalcites were prepared with the Cu:Zn ratio varying from 6:0, 4:2, 3:3, 2:4 and 0:6. The concentrations of the Cu^{2+} and Zn^{2+} were varied accordingly. Solution 2 in the appropriate ratio was added to solution 1 using a peristaltic pump at a rate of 40 cm^3/min, under vigorous stirring, maintaining a pH of 10.

2.2. Thermal analysis

Thermal decomposition of the hydrotalcite was carried out in a TA® Instrument incorporated high-resolution thermogravimetric analyser (series Q500) in a flowing nitrogen atmosphere (80 cm^3/min). Approximately 50 mg of sample was heated in an open platinum crucible at a rate of 2.0 °C/min up to 500 °C. With the quasi-isothermal, quasi-isobaric heating program of the instrument the furnace temperature was regulated precisely to provide a uniform rate of decomposition in the main decomposition stage. The TGA instrument was coupled to a Balzers (Pfeiffer) mass spectrometer for gas analysis. Only selected gases were analysed.

Differential scanning calorimetry (DSC) was performed on a TA® Instrument DSC Q10 analyser. Sample powders were loaded into sealed alumina pan and heated to 500 °C at heating rate of 2 °C/min. The empty alumina pan was used as reference and the heat flow between the sample and reference pans was recorded.

3. Results and discussion

3.1. Differential scanning calorimetry

The formulae of the hydrotalcites may be likened to a solid solution series with the end members being ($Cu_6Al_2(OH)_{16}(CO_3)\cdot 4H_2O$) and ($Zn_6Al_2(OH)_{16}(CO_3)\cdot 4H_2O$). In this work, this latter end member is not strictly relevant to the current study for the synthesis of nano-composites for the potential photo-oxidation of organics in aqueous media. The results are shown for completeness. The minerals were checked for purity and hydrotalcite formation using X-ray diffraction. Minerals, such as the synthesised hydrotalcites decompose at low temperatures and are ideal for measurement by DSC. Fig. 1 displays the analyses of the Cu/Zn hydrotalcites and the results of the peak fitting of the analyses are reported in Table 1. The data shown in this table reports the peak temperatures and displays the complete band component analysis of the DSC curves. The small steps may well be artefacts generated by the computer fitting program. However, such small steps may be of significance when small changes in the thermal analysis patterns are being studied. Both the figure and the table clearly show that the thermal decomposition is complex with many overlapping heat flow steps. Fig. 1 clearly shows two major endothermic reactions at around 140–170 °C and at around 230 °C. The peaks are strongly asymmetric on the low temperature side and as a consequence, steps 4–7 make up the first peak and steps 8 and 9 make up the second peak.

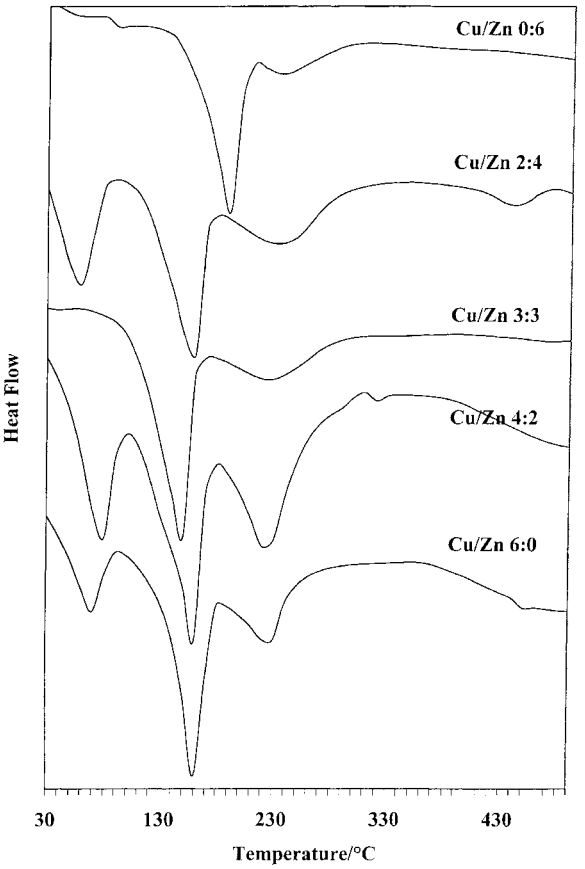

Fig. 1. Differential scanning calorimetry of Cu/Zn hydrotalcites.

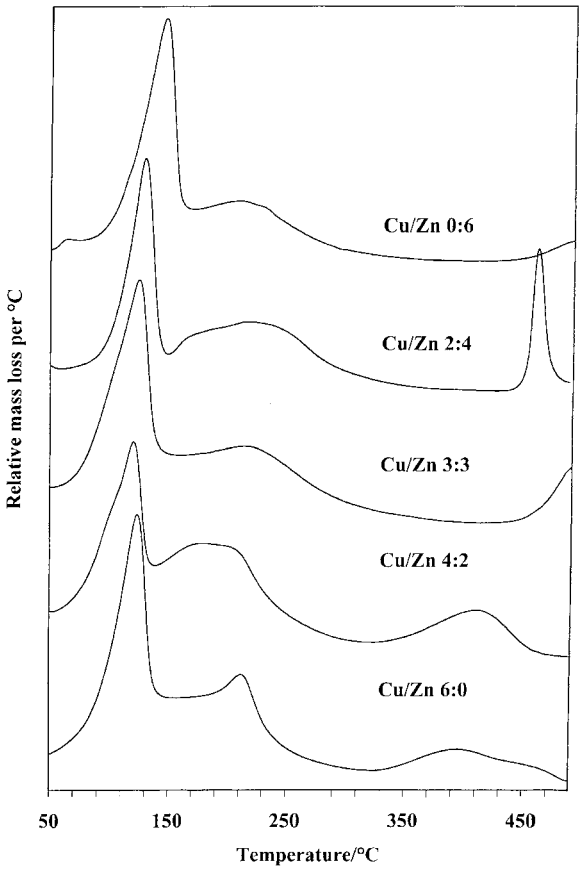

Fig. 2. High resolution DGTA of Cu/Zn hydrotalcites.

Table 1
Results of the DSC for Cu/Zn/Al hydrotalcites

Heat flow step	Cu/Zn hydrotalcites (°C/%)				
	Cu:Zn 6:0	Cu:Zn 4:2	Cu:Zn 3:3	Cu:Zn 2:4	Cu:Zn 0:6
Step 1	50/0.7	58/1.3	32/0.1	50/8.8	59/0.3
Step 2	65/1.2	71/1.2	41/0.2	62.8/2.2	91/0.2
Step 3	74/2.8	81/6.1	99/2.2		104/2.8
Step 4	147/14.9	131/12.4	127/8.9	140/11.1	132/0.6
Step 5	156/5.1	149/4.3	140/4.7	145/13.2	162/6.0
Step 6	163/2.8	159/3.0	147/6.4	153/5.5	178/10.1
Step 7	167/1.0	164/1.1	152/1.7	160/2.4	188/7.7
Step 8	201/2.3		184/5.4	163/0.4	194/2.3
Step 9	229/38.5	212/43.4	230/21.4	227/38.4	234/22.7
Step 10				415/9.9	
Step 11	440/5.2		445/2.7	441/6.7	

It is convenient to subdivide the data in accordance with the temperature range: (a) steps below 110 °C, (b) steps from 110 to 200 °C, and (c) steps between 200 and 300 °C and steps above 300 °C.

The ($Cu_6Al_2(OH)_{16}(CO_3)\cdot 4H_2O$) end member shows heat flow steps at 50, 65 and 74 °C which may be attributed to the dehydration of the hydrotalcite from water adsorbed on the outside of the anionic clay or as is more likely between the anionic clay layers. The percentage heat flow of these steps depends on the degree of dryness in the preparation of the hydrotalcite. Such variation is observed for the hydrotalcites: $Cu_4Zn_2Al_2(OH)_{16}(CO_3)\cdot 4H_2O$, $Cu_3Zn_3Al_2(OH)_{16}(CO_3)\cdot 4H_2O$, $Cu_2Zn_4Al_2(OH)_{16}(CO_3)\cdot 4H_2O$. In general, as the Cu is substituted by the Zn, the temperature of the dehydration steps shifts to slightly higher temperatures.

The question arises as to why there is several heat flow dehydration steps. The hydrotalcite structure is based upon the brucite structure such that some of the Mg is replaced by Al. In other words, $Mg(OH)_2\cdot xH_2O$ becomes $Mg_6Al_2(OH)_{16}(CO_3)\cdot 4H_2O$. In this case, we have replaced the Mg entirely by Cu or Cu_xZn_{6-x}. A number of questions arise as to the siting of the Cu and Al in the hydrotalcite structure and also the Cu, Zn and Al in the hydrotalcite layered structure. Are the aluminium cations well separated by the Mg or do the cations form aggregations of Cu, Zn and Al in the layers? The observation of several heat loss steps in the temperature range up to 104 °C suggests that the water is adsorbed differently on the CuOH, ZnOH and AlOH units. The observation of several heat flow steps for the $Cu_xZn_{6-x}Al_2(OH)_{16}(CO_3)\cdot 4H_2O$ hydrotalcites suggests that aggregations or 'lakes' of Cu and Zn may be formed in the LDH structure since the adsorbed water is being lost at a number of temperatures.

A major heat flow step is observed for the $Cu_xZn_{6-x}Al_2(OH)_{16}(CO_3)\cdot 4H_2O$ hydrotalcites in the 127–201 °C (heat flow steps 4–8). The major enthalpy change is in the temperature range of 147–150 °C. Variation in the amount of heat flow and the temperature of the phase loss appears to be a function of the degree of substitution of the Cu by Zn. These enthalpy steps are attributed to the loss of the hydroxyl units from the hydrotalcite sheets. Two higher temperature enthalpy changes are observed at around 230 and at 440 °C. The heat flow step at 230 °C is ascribed to the loss of the interlayer anion (carbonate) and as will be shown later in this paper is confirmed by the mass spectrometric analysis of evolved carbon dioxide gas. The higher temperature heat flow step is also attributed to the loss of carbon dioxide. It is suggested that as the hydrotalcite dehydroxylates and decarbonates, some of the carbonate ions is forced to bond to the cations and form molecules, such as $CuCO_3$ and $ZnCO_3$. The percentage heat flow of this

Table 2
Results of the weight losses of the DTG and MS for Cu/Zn/Al hydrotalcites

Weight loss step	Hydrotalcites (°C/%)									
	Cu:Zn 6:0		Cu:Zn 4:2		Cu:Zn 3:3		Cu:Zn 2:4		Cu:Zn 0:6	
	DTG	MS	DTG	MS	DTG	MS	DTG	MS	DTG	MS
Step 1	30/0.1	30/2.7	29/4.9	30/1.1	24/7.5	32/0.2	33/8.0	22/19.9	26/0.7	28/0.2
Step 2			76/3.5	79/0.4					64/0.2	67/0.5
Step 3	106/10.5	110/28.6	103/15.4	105/33.4	106/22.4	101/21.4	113/13.2	113/19.2	100/13.7	119/3.8
Step 4	117/11.3	120/14.5	117/4.1	117/12.5	120/6.4	118/19.3	121/11.6	125/9.0	124/10.4	135/39.5
Step 5	126/5.1	127/6.1	123/2.4	123/5.4	127/3.5	127/7.7	131/8.8	132/5.2	135/5.5	147/13.9
Step 6	156/50.2	141/1.6	177/42.6	176/44.0	154/29.5	138/8.6	165/2.0	160/8.1	142/13.3	155/6.0
Step 7	188/3.8	165/34.9					176/0.9	171/6.1	149/6.2	181/3.7
Step 8							184/1.7	181/3.8		
Step 9							194/1.9	198/11.0		
Step 10	213/7.4	213/20.5	210/1.4	212/22.0	223/25.7	221/65.6	210/5.6	205/16.6	203/42.9	201/26.4
Step 11			247/8.3	257/34.2			238/35.4	247/15.1	228/3.3	225/27.0
Step 12	396/9.5	379/30.0	382/7.8	360/1.7						
Step 13	458/2.1	433/12.9	415/4.5	401/23.0			457/2.5	442/0.8		
Step 14			433/1.8	447/0.2	490/4.9	495/26.3	461/8.4	459/24.0	490/3.9	491/0.3

step is low and it is evident that the heat flow step is only secondary.

3.2. High resolution thermogravimetric analysis

The DTG curves of the high-resolution thermogravimetric analyses of the $Cu_xZn_{6-x}Al_2(OH)_{16}(CO_3)\cdot 4H_2O$ hydrotalcites are shown in Fig. 2. The results of the analysis of these DTG curves are reported in Table 2. Included in this table for comparison is the percentage weight loss as measured from the evolved gas mass spectrometry. The temperatures listed in the table are peak temperatures. The percentage weight loss in the steps represents the integral of the DTG curves and is the percentage of the total mass loss. In many respects, the DTG patterns follow the DSC patterns. The heating rates are however, significantly different which may make any comparison questionable. The data may be analysed in a similar fashion to that of the DSC. The weight loss steps may also be divided into below 120 °C and above 120 °C. The weight loss below 80 °C is assigned to adsorbed water. The values here are difficult to determine because the DTG curve comes off a very steep almost vertical line, and as a consequence base line fitting is difficult. Three weight loss steps are observed in the temperature range of 100–140 °C. The theoretical weight loss for a hydrotalcite of formula ($Cu_6Zn_0Al_2(OH)_{16}(CO_3)\cdot 4H_2O$) is approximately 8.58% for H_2O, 5.24% for CO_2 and 17.16% for the OH units.

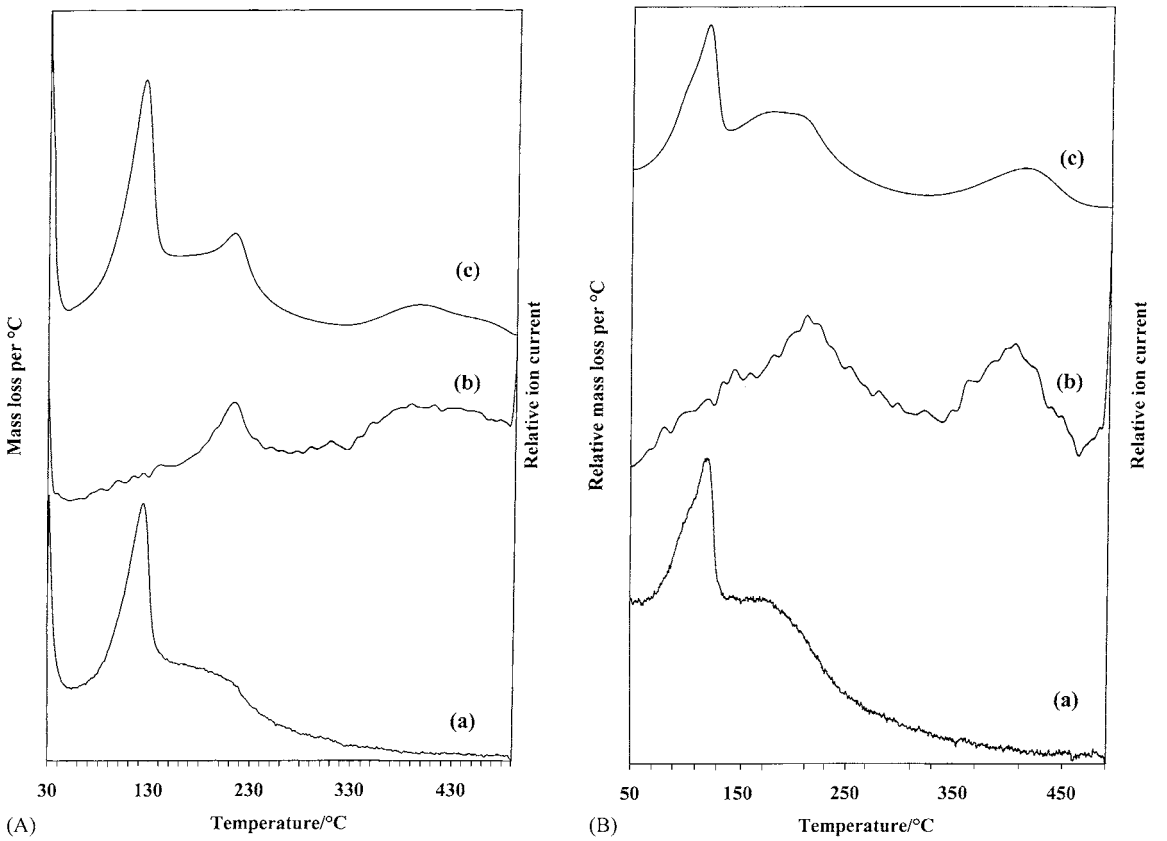

Fig. 3. (A) MS of evolved water vapour (curve a), MS of evolved CO_2 (curve b), and DTG curve for Cu/Al hydrotalcite (curve c); (B) MS of evolved water vapour (curve a), MS of evolved CO_2 (curve b), and DTG curve for 4:2 Cu–Zn/Al hydrotalcite (curve c); (C) MS of evolved water vapour (curve a), MS of evolved CO_2 (curve b), and DTG curve for 3:3 Cu–Zn/Al hydrotalcite (curve c); (D) MS of evolved water vapour (curve a), MS of evolved CO_2 (curve b), and DTG curve for 2:4 Cu–Zn/Al hydrotalcite (curve c); (E) MS of evolved water vapour (curve a), MS of evolved CO_2 (curve b), and DTG curve for Zn/Al hydrotalcite (curve c).

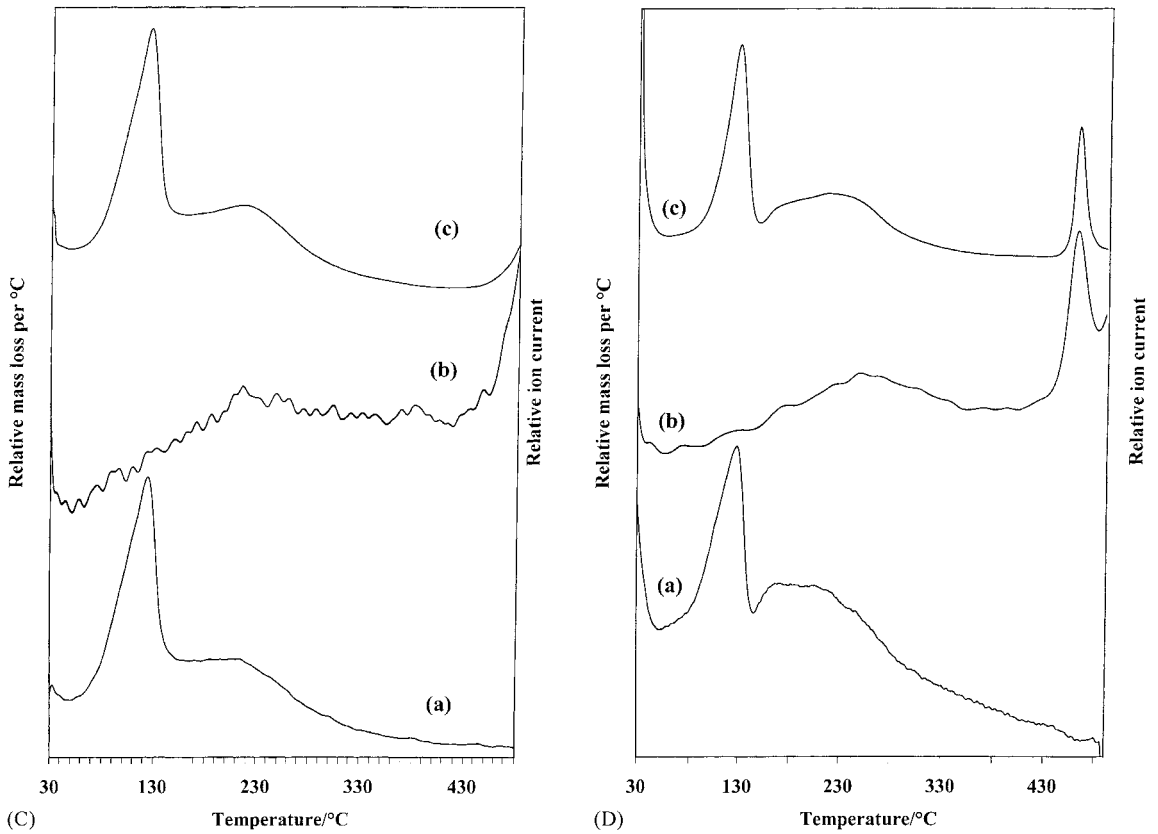

Fig. 3. (*Continued*).

The theoretical weight losses for the Zn substituted copper hydrotalcites will be to a first approximation the same. The total theoretical weight loss for these three steps is 31%. The sum of the weight losses for the three steps (steps 3–5 in Table 2) involving the weight loss of: (a) water, (b) CO_2, and (c) hydroxyls as H_2O is 26.9, 21.9, 35.3 and 33.2 for the hydrotalcites of ratios 6:0, 4:2, 3:3, 2:4, respectively. These values are in general less than the theoretical value of 31%. What this means is that some of the hydroxyls are retained to higher temperatures and are lost simultaneously with the CO_2. The weight loss for step 6 is assigned to the loss of carbonate and a large value is noted for this step. This value may be an artefact of the curve fitting procedure because of the broad background and as such should be discounted. Higher temperature weight loss steps are observed around 210 °C and are assigned to a further loss of carbonate. A further weight loss steps is observed around 400 °C and is assigned to the further loss of carbonate chemically bonded to the cations.

3.3. Mass spectrometric analysis

The results of the mass spectra analyses of the four hydrotalcites of evolved water vapour and carbon dioxide are shown in Fig. 3. The results of the mass loss as determined by mass spectrometry are reported in Table 2. This table also compares the mass losses as measured by mass spectrometry and the weight losses as determined by differential thermogravimetric analysis. The temperatures listed in the table are peak temperatures. The percentage mass loss in the steps represents the integral of the MS curves and is the percentage of the total mass loss. It is a fundamental principal that the mass spectrometric curves follow the

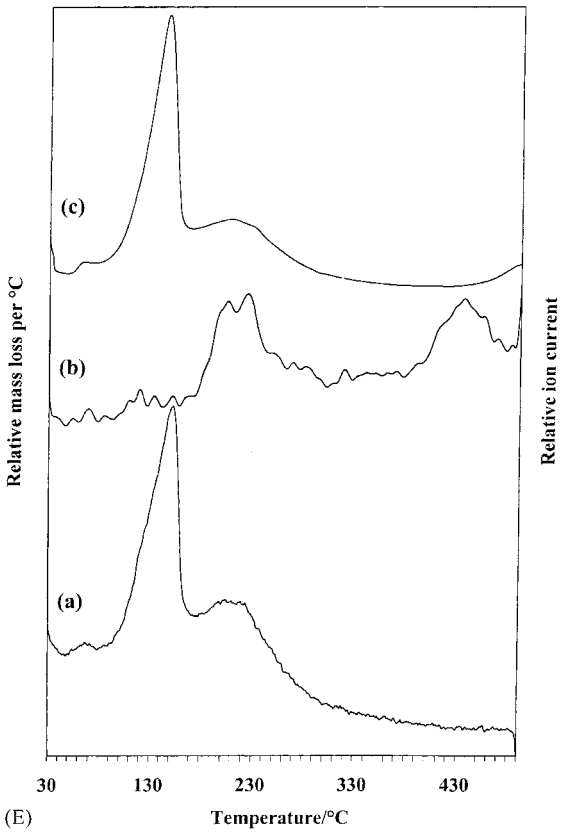

Fig. 3. (*Continued*).

DTG curves. This is the exacted in by comparing the sum of the curves a and b with c in Fig. 3A. This figure clearly shows that the water comes off in three steps at 110, 120 and 165 °C. The carbon dioxide is lost in two steps at 213 and 379 °C. The first carbonate loss step overlaps with the last dehydroxylation step. This simultaneous loss of OH and carbonate units fits well with recent infrared data, which has shown that the carbonate is strongly bonded to the interlayer water and to the hydroxyl units in the structure. Similar patterns are observed for the Cu/Zn 4:2 and 3:3 hydrotalcites. For the 6:0 hydrotalcite an additional loss of carbonate is observed at 430 °C. This result is in harmony with both the DSC and high resolution DTG results where similar effects were observed. This high temperature mass loss is also observed in Fig. 3E and it is concluded that the mass loss of carbonate is due to bonding of the carbonate to the zinc cation.

Recent studies of a complex hydrotalcite based upon CuCoZnAl layered double hydroxides (LDHs) with various Cu/Co atom ratios showed that using thermal analyses of materials indicated three stages of endothermic weight loss processes due to the loss of interlayer H_2O and some loosely bound CO_3^{2-} (100–250 °C), loss of structural H_2O and CO_3^{2-} (250–400 °C) and the loss of some strongly held CO_3^{2-} anions (above 500 °C) [16]. These results are in good agreement with our data. Other work has shown that for Cu/Zn/Co/Cr hydrotalcites the thermal analysis results were independent of the cation [17]. Such a concept is different to what has been reported in this research. Here, we find that the thermal analyses both DSC and DTG coupled to MS are cation dependent and that the thermal analysis steps are cation mole ratio dependent.

4. Conclusions

A series of copper based aluminium-hydrotalcites of formulae $Cu_{6-x}Zn_xAl_2(OH)_{16}(CO_3)\cdot 4H_2O$ with zinc substitution have been studied by a combination of DSC and high resolution thermogravimetry in combination with an evolved gas mass spectrometer. DSC shows that increased substitution of the Cu by Zn results in the shift of the heat flow steps to higher temperature. The endotherms are complex with overlapping endothermic steps suggesting that some cation ordering occurs in the hydrotalcite structure. More steps are observed in the DSC patterns than for the DTG. This suggests that some of the endothermic steps are surface phase related involving changes in the hydroxyl surface structure.

High resolution DTG combined with mass spectrometry shows that the temperature of the dehydroxylation of the $Cu_{6-x}Zn_xAl_2(OH)_{16}(CO_3)\cdot 4H_2O$ hydrotalcite increases with increased Zn composition. The principal weight loss steps observed are (a) loss of adsorbed and interlayer water in the temperature range of 40–50 °C, (b) loss of hydroxyls between 110 and 150 °C, (c) dehydroxylation in the 200–250 °C with associated carbon dioxide loss, and (d) loss of carbonate in the temperature range of 400–450 °C. The results of these thermal analyses show that hydrotalcites are well suited for the inclusion in nano-composites. The temperature of decomposition

is well suited for the synthesis of mixed metal oxides on a molecular scale such that the copper oxide based nano-composites are useful in the photo-oxidation of organics in aqueous systems.

References

[1] E.A. Karakhanov, S.V. Kardashev, L.L. Meshkov, S.N. Nesterenko, Vestn. Mosk. Univ., Ser. 2: Khim. 39 (1998) 214.
[2] J. Bandara, J. Kiwi, C. Pulgarin, G. Pajonk, J. Mol. Catal. A: Chem. 111 (1996) 333.
[3] H. Gomez, R. Schrebler, R. Cordova, Casanova Y, P. Velasquez, Bol. Soc. Chil. Quim. 42 (1997) 207.
[4] Y. Ichihashi, Y. Matsumura, J. Catal. 202 (2001) 427.
[5] S.A.A. Mansour, J. Therm. Anal. 45 (1995) 1381.
[6] B.V. L'vov, A.V. Novichikhin, Spectrochim. Acta Part B 50B (1995) 1459.
[7] J.G. Jackson, A. Novichikhin, R.W. Fonseca, J.A. Holcombe, Spectrochim. Acta Part B 50B (1995) 1423.
[8] T.P. El'tsova, A.A. Kotsyuba, V.D. Parkhomenko, Vopr. Khim. Khim. Tekhnol. 62 (1981) 100.
[9] L. Hickey, J.T. Kloprogge, R.L. Frost, J. Mater. Sci. 35 (2000) 4347.
[10] J. Theo Kloprogge, R.L. Frost, Appl. Catal. A 184 (1999) 61.
[11] J. Theo Kloprogge, R.L. Frost, Phys. Chem. Chem. Phys. 1 (1999) 1641.
[12] R.H. Hoeppener, E.B.M. Doesburg, J.J.F. Scholten, Appl. Catal. 25 (1986) 109.
[13] F. Kovanda, K. Jiratova, J. Rymes, D. Kolousek, Appl. Clay Sci. 18 (2001) 71.
[14] C.W. Beck, Am. Mineralogist 35 (1950) 985.
[15] G.W. Brindley, S. Kikkawa, Clays Clay Miner. 28 (1980) 87.
[16] S. Velu, K. Suzuki, S. Hashimoto, N. Satoh, F. Ohashi, S. Tomura, J. Mater. Chem. 11 (2001) 2049.
[17] P. Porta, S. Morpurgo, Appl. Clay Sci. 10 (1995) 31.